DOI: 10.1002/chem.200902199

Vibrational Signature of Double-End-Linked Molecules at Au Nanojunctions Probed by Surface-Enhanced Raman Spectroscopy

Yi-Fan Huang, Nai-Ning Yin, Xiang Wang, De-Yin Wu,* Bin Ren,* and Zhong-Qun Tian[a]

In the past decade, a lot of efforts have been made to look for new materials and develop new methods for molecular electronic devices. Metal/molecule/metal junctions have been widely used as a model system for discovering new devices and studying the working principle of the molecular devices. Up to date, molecular rectifiers, wires, and switches have been reported on the basis of the above strategy.[1] However, the mechanism of the electron transport in molecular devices still remains ambiguous due to a lack of understanding of the molecular structure in the junction, especially during the conducting process; this has become a severe barrier for the development of molecular devices. Therefore, it is highly desirable to develop strategies capable of identifying and characterizing the structure of molecules in the junction to reveal the relationship between the electrical properties and the molecular structure, one of the most important issues in the molecular electronics. Among various techniques for characterizing molecular junctions, vibrational spectroscopy appears to be very powerful and promising because it can readily provide the structural information at the molecular level. For example, inelastic electron tunneling spectroscopy,[2a,b] infrared,[2c,d] and surface-enhanced Raman spectroscopy (SERS)[2e–h] have been utilized to characterize the molecules trapped in the junctions.

Among them, SERS is particularly suitable for this purpose owing to its ultra-high sensitivity to single molecules, non-destructivity for diagnosing the trace amount of surface species, and the capability of working in the normal environment, in addition to the abundant information on the molecular structure.[3] The huge enhancement obtained in the single molecule SERS reveals the importance of the electromagnetic coupling (mainly localized surface plasmon resonance, LSPR) between nanoparticles (NPs), which is the physical origin of hot spots. The molecules sitting in the vicinity of a hot spot will experience the most significant enhancement. Among these molecules, some of them may bridge between the two NPs, forming the important metal/molecule/metal junction. The molecules in such a configuration are termed double-end-bonded (DB) species. In normal SERS measurements, the coverage of surface species amounts to a full monolayer. Therefore, the relative number of DB species to the single-end-bonded (SB) species is relatively low. As a result, the signal from DB species may be merged with that of the SB species, even though most DB species experience the highest enhancement.

In this work, we propose a strategy to overcome this problem, the schematic diagram of which is shown in Figure 1a. As can be seen in the figure, when bare Au NPs are dispersed on a smooth Au electrode adsorbed with a monolayer of target molecules, for example, 4,4′-bipyridine (bpy) or 1,4-benzenedithiol (bdt), the important metal/molecule/metal junctions will naturally form on the surface. In this case, those molecules adsorbed on the smooth Au surface and which are not in close vicinity to the NPs will not give any detectable SERS signal, so that we can effectively eliminate the background signal. On the other hand, the coupling between the NPs with the electrode may markedly enhance the electromagnetic field and therefore the Raman signal of the molecules in vicinity of the junction will be significantly enhanced.[4] In this case, the ratio of the signals of the DB to SB species significantly increases so that the signal in the junctions can be manifested. The finite-difference time-domain (FDTD) calculation was performed to estimate the field enhancement in the nanojunction system and density functional theory (DFT) was utilized to analyze the relationship between the Raman spectral feature and the structure

[a] Y.-F. Huang, N.-N. Yin, X. Wang, Prof. Dr. D.-Y. Wu, Prof. Dr. B. Ren, Prof. Dr. Z.-Q. Tian
State Key Laboratory for Physical Chemistry of Solid Surfaces and Department of Chemistry
College of Chemistry and Chemical Engineering
Xiamen University, Xiamen, 361005 (China)
Fax: (+86) 592-2186979
E-mail: bren@xmu.edu.cn
dywu@xmu.edu.cn

Supporting information for this article is available on the WWW under http://dx.doi.org/10.1002/chem.200902199.

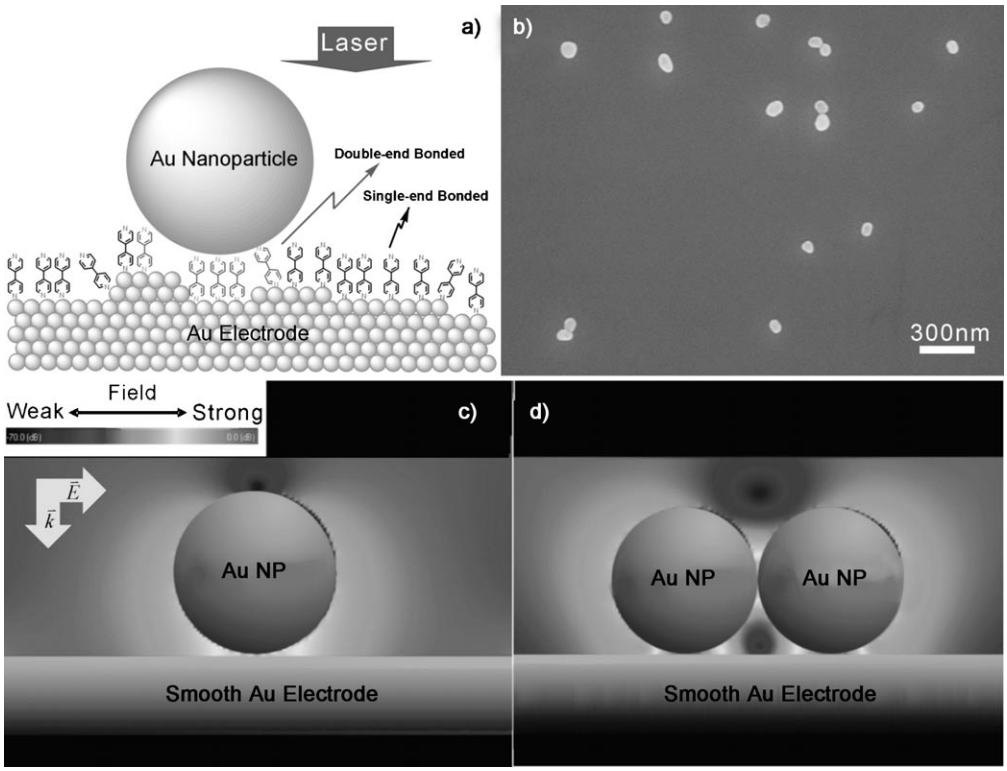

Figure 1. The architecture (a) and an SEM image (b) of the Au/bpy/Au junction and the distribution of the electromagnetic field of the monomer of an Au sphere (c) and the dimer (d) on a smooth Au electrode simulated by FDTD.

of the molecule. This work provides a feasible strategy for investigating the structure of molecules in the junction by SERS.

Figure 1b presents the SEM image of the self-assembled Au NPs on the Au electrode adsorbed with bpy. The coverage of the NPs is much less than a monolayer. It can be easily understood from the schematic diagram of Figure 1a that the molecular number ratio of DB to SB species increases with the increase of the coverage of the NPs. In general, because the size of the NPs is much larger than that of the molecule, it is highly possible that there may be one to several molecules trapped in the junction of the NPs and the electrode, which will further increase the ratio. Evidently, the absolute amount of the SB species should always be larger than that of DB species. However, in such a configuration, only those molecules trapped in the junction can be greatly enhanced through LSPR coupling between the NPs and the electrode and SB molecules will experience exponentially decreasing enhancement with the increase of the distance to the junction.[5] To understand such a statement, Figure 1c depicts the distribution of the electric field simulated by FDTD method for a configuration of single NP with a Au electrode. It can be seen that the enhancement is constrained in the junction between the NP and the electrode and decays exponentially with the increase of the distance to junction. In the SEM image (Figure 1b) we see that some NPs form dimers. To consider how the formation of dimer will influence the distribution of the field strength, we simulated the configuration of the dimer on the smooth Au electrode and the result is shown in Figure 1d. Surprisingly, the junction of the NPs and the electrode gives about 600-fold enhancement over that in junction of the two NPs. The enhancement in the former junction is about 2–3 orders of magnitude higher than that in other region of the surface. Considering the increasing amount of molecules contributing to the total signal with the increasing distance away from the centre of the junction, we estimated the intensity ratio of DB to SB according to the FDTD results mentioned above (see Supporting Information for detailed method). The contrast of DB/SB for monomer and dimer is about 0.015 and 0.327, respectively. From the FDTD result, the intensity ratio of DB obtained in the dimer to monomer cases is about 3.5×10^4 (see the Supporting Information for details). In Figure 1b, we see that the number of dimers is only about one third of that of the monomers. Therefore, one can easily find out that it is the dimer instead of the monomer that contributes to the side band at 1645 cm^{-1} and the small amount of DB molecules can give comparable intensity to that of a large amount of SB molecules.

Figure 2a and 2b shows the Raman spectra of bpy on a roughened Au electrode and on the molecular junction of Au electrode/bpy/Au NPs. The signal-to-noise ratio of Au/bpy/Au is lower than that of bpy on the roughened Au electrode. This phenomenon is understandable and can be ascribed to a much lower number of junctions in the Au/bpy/Au case compared with the large amount of aggregates on

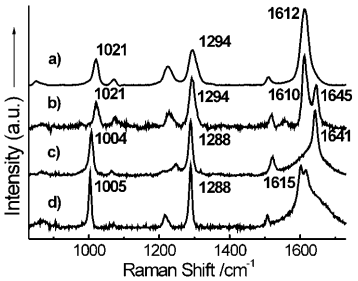

Figure 2. Raman spectra of bpy on a) roughened Au, b) Au/bpy/Au, c) in acidic and d) in neutral aqueous solution.

the roughened Au substrate. The bands at about 1021, 1294, and 1610 cm^{-1} dominate the spectra profile with similar relative intensity in both spectra. A new band at 1645 cm^{-1}, which has not been observed in any previously reported SERS spectrum, appears in the spectrum of the Au/bpy/Au. Interestingly, in our previous tip-enhanced Raman spectroscopic study of bpy on a Au(111) surface, a similar band at 1635 cm^{-1} was observed, which was ascribed to the bpy lying flat on the surface and connected by protons assisted by the simultaneously obtained STM image.[6] So we speculate that the band at 1645 cm^{-1} in the present system might arise from the bpy bonded to the Au electrode and the Au NPs simultaneously. In order to verify the speculation, the Raman spectra of bpy and its diprotonated species the bonding configuration of which is similar to that of Au/bpy/Au were studied. Figure 2c and 2d shows the Raman spectra of bpy in neutral ($pH \approx 6.4$) and acidic ($pH < 1$) aqueous solutions. A frequency shift from 1615 to 1641 cm^{-1} is observed. A similar protonation effect has been reported in the literature.[7] Hence, we think the appearance of the 1645 cm^{-1} band is very likely due to the bonding effect on both nitrogen atoms in the two pyridyl rings, which can be considered as a characteristic of the junction configuration.

In order to study the influences of the bonding effect on the SERS spectra and the structure of the molecular junction, we performed DFT calculation of the Raman spectra of DB bpy with the Au_1 or Au_4 clusters. Previous theoretical and experimental results indicate that bpy can be chemisorbed strongly on the substrate. Therefore, the system can be well described by the cluster model. A change in the molecular structure may indicate the influence of the bonding effect with the formation of junctions. Unfortunately, we cannot find any significant difference between the bpy/Au_4 and the Au_4/bpy/Au_4, as shown in Figure S2 in the Supporting Information. Besides, the calculated spectrum of SB bpy/Au_4 is similar to that of DB Au_4/bpy/Au_4, although a small shoulder band appearing at 1597 cm^{-1}, which is assigned to the υ_{8a} mode of the non-bonded pyridyl ring.[8] To understand the deviation between the theoretical and experimental work, we calculated the vibrational frequencies of bpy and $bpyH_2^{2+}$. Interestingly, the calculated band position of the υ_{8a} mode of bpy shifts from 1605 to 1642 cm^{-1} when it is diprotonated (See Supporting Information). It fits the experimental result very well. Considering the polarization effect of the protons in $bpyH_2^{2+}$, we further calculated the $(Au/bpy/Au)^{2+}$ cluster. Compared to bpy–Au (1607 cm^{-1}), the υ_{8a} band frequency of $(Au/bpy/Au)^{2+}$ cluster shifts to a higher frequency (1617 cm^{-1}). However, when the size of the Au clusters increases, the shift diminished markedly. We speculate that it can be ascribed to the charge redistribution in the larger clusters. However, the present results imply that the localization of charge may be a key character of molecular junctions.

Next, we examined the bonding effect on the electronic structure of bpy. Under the harmonic approximation, the frequency of a Raman active mode is determined by the reduced mass and the force constant. The bonding effect can affect the frequency of a vibrational mode by strengthening or weakening the correlated bond. Comparing the molecular orbitals of bpy and $bpyH_2^{2+}$, we find that the bonding effect readily affects the π^* orbital distribution between C2 and C3, C5 and C6, C2′and C3′, and C5′and C6′ (as shown in Figure 3top and bottom right), which contribute primarily to

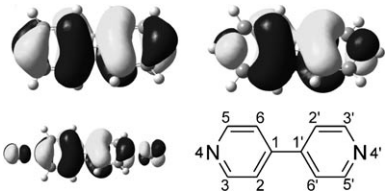

Figure 3. The correlated molecular orbitals of bpy (top left), $bpyH_2^{2+}$ (top right), $(Au/bpy/Au)^{2+}$ (bottom left) and the notation of the atoms of bpy (bottom right).

the υ_{8a} mode. Similarly, the orbital can also be influenced by the bonding of Au atoms in $(Au/bpy/Au)^{2+}$ as shown in Figure 3 (bottom left). In fact, bpy is a heterocyclic aromatic species and the hybridization of the nitrogen atom is sp^2. The two $2p_z$ orbitals of nitrogen atoms form a conjugated π orbital with carbon atoms. The attachment of Au atom to the nitrogen atoms of bpy reduces the antibonding feature of the occupied π orbital between C2 and C3. In addition, the electrostatic interaction induces the redistribution of the electron density as displayed in Figure 3 (bottom left). Both of the above two factors strengthen the C2–C3 bond, so the frequency of the υ_{8a} mode increases due to the strengthening of the bond.

To confirm the above results, we selected 1,4-benzenedithiol (bdt), another important model molecule in the investigation of molecular devices, as a linking molecule. Being different from the heterocyclic aromatic structure, bdt is a *para*-derivative of di-substituted benzene and the binding group is not directly on the aromatic ring.

Figure 4 (left) displays the SERS spectra of bdt on a roughened Au and Au/bdt/Au junctions. Again, it is observed that the signal-to-noise ratio of Au/bdt/Au is lower in the latter case; however, both of the spectral profiles are dominated by the bands at 1064, 1175, and 1564 cm^{-1}. The frequencies of the υ_{8a} mode or other bands do not show ob-

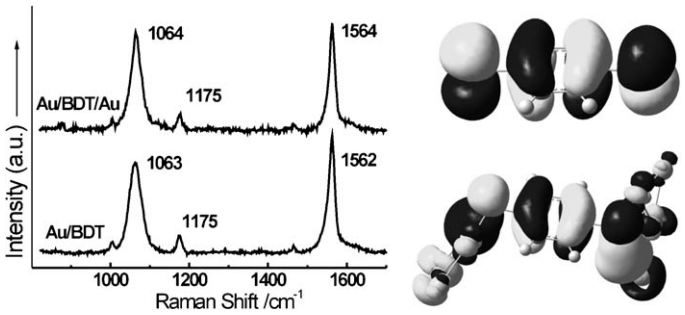

Figure 4. Left: The SERS spectra of bdt on Au/bdt/Au (upper spectrum) and a roughened Au electrode (lower spectrum). Right: the correlated π* orbital of bdt (top) and Au_5/bdt/Au_5 (bottom).

servable shift by the bonding effect. According to the previous analysis of bpy, we examined the bonding effect on the π* orbital of bdt. As shown in Figure 4 (right), the bonding of two Au clusters to bdt has a minor effect on the distribution of that orbital. In fact, bdt attaches to the Au atom through its sulfur atom. The localized bond between Au and S prevents the influence of Au on the phenyl ring.[9] As a result, the bonding effect on the benzene ring is much smaller than that on the pyridyl ring. Therefore, the influence from bonding effect on the vibrational spectrum of bdt is too weak to be observed. Furthermore, this result also demonstrates that the heterocyclic aromatic species the aromatic ring of which bonds to the metal electrode directly in metal/molecule/metal junctions can be identified by SERS according to the frequency of the vibration in aromatic rings.

In summary, we conveniently obtained a large number of Au/bpy/Au and Au/bdt/Au junctions by spreading Au NPs over a smooth Au electrode pre-adsorbed with molecules with bifunctional groups. The molecular junctions were successfully identified and characterized by SERS. We found that the frequency shift of the υ_{8a} mode (from 1610 to 1645 cm^{-1}) of bpy can be used as a signature to verify the formation of Au/bpy/Au junction. The comparative study of bpy and bdt indicates that it is better to choose molecules that have a very sensitive response to the bonding effect, such as bpy rather than bdt, in order to study the structure of molecules in the junction. The results also indicate that SERS can be used as an effective tool for identifying and characterizing the molecules in junctions by spreading clean SERS-active nanoparticles over a functional molecule-modified planar substrate.

Experimental Section

Experimental methods: Spherical Au NPs with a diameter of 55 nm were synthesized by reducing $HAuCl_4$ with sodium citrate according to the procedure reported in the literature.[10] The junctions were prepared according to the following procedure: mechanically polished mirror-finish Au electrodes were immersed into the 1 mM solution of bpy in water or bdt in ethanol for 20–30 min. Then, they were rinsed with the respective solvents so that the physically adsorbed molecules on the surface can be removed leaving the self-assembly monolayer. Afterwards, the diluted Au sol (nearly colorless) was dropped onto the smooth Au electrodes surfaces adsorbed with target molecules, which was let dry in vacuum to obtain the desired Au nanoparticle/molecule/smooth Au electrode junctions.

Computational methods: The cluster models with sizes of Au_1, Au_4, and Au_5 were selected to simulate the surface of electrode or NPs. The calculations were performed by hybrid density functional of B3LYP[11] for full geometry optimizations and vibrational spectral calculations. The basis sets for C, N, S and H were 6-311+G**. The valence and core electrons of Au were described by LanL2DZ and its ECP, respectively.[12] The method has been safely used to predict the bonding energy and the vibrational spectra between pyridine and Au cluster.[13] In order to fit the experiment, the frequency was scaled by a factor of 0.98. All the calculations were performed with the software package Gaussian 03.[14] The electromagnetic field distribution was simulated by the 3D-FDTD method by using X-FDTD software by numerically solving Maxwell's functions.[15] . The EM enhancement was estimated based on the result. The substrate was modelled as an Au nanoparticle dimer with 1 nm interparticle distance on an Au film. According to the experiment condition, the dimer was also set at distance of 1 nm away from the film. The wavelength dependent dielectric constants of Au NPs was derived from the experimental results.[16] The 632.8 nm excitation line irradiated perpendicular to the axis connecting two particles with a parallel polarization. The Yee cell size was 1×1×1 nm. The total number of time steps was 35000 to ensure convergence.

Acknowledgements

This work was supported by National Basic Research Program of China (973 Program No. 2009CB930703, 2007CB935603 and 2007DFC40440), Natural Science Foundation of China (20673086, 20620130427, 20825313, and 20827003), and NFFTBS (J0630429). D.Y.W. thanks the financial support from NCETFJ and HPC of Xiamen University.

Keywords: gold · molecular junctions · nanoparticles · Raman spectroscopy · self-assembly

[1] a) C. Zhou, M. R. Deshpande, M. A. Reed, L. Jonesll, J. M. Tour, *Appl. Phys. Lett.* **1997**, *71*, 611–613; b) R. M. Metzger, *Chem. Rev.* **2003**, *103*, 3803–3834; c) X. D. Cui, A. Primak, Z. Zarate, J. Tomfohr, O. F. Sankey, A. L. Moore, T. A. Moore, D. Gust, G. Harris, S. M. Lindsay, *Science* **2001**, *294*, 571–574; d) B. Xu, N. J. Tao, *Science* **2003**, *301*, 1221–1223; e) D. Gosztola, M. P. Niemczyk, M. R. Wasielewski, *J. Am. Chem. Soc.* **1998**, *120*, 5118–5119; f) D. Dulic, S. J. van der Molen, T. Kudernac, H. T. Jonkman, J. J. D. de Jong, T. N. Bowden, J. van Esch, B. L. Feringa, B. J. van Wees, *Phys. Rev. Lett.* **2003**, *91*, 207402.

[2] a) J. G. Kushmerick, J. Lazorcik, C. H. Patterson, R. Shashidhar, D. S. Seferos, G. C. Bazan, *Nano. Lett.* **2004**, *4*, 639–642; b) W. Wang, T. Lee, I. Kretzschmar, M. A. Reed, *Nano. Lett.* **2004**, *4*, 643–646; c) Y. Jun, X. Y. Zhu, *J. Am. Chem. Soc.* **2004**, *126*, 13224–13225; d) B. de Boer, M. M. Frank, Y. J. Chabal, W. Jiang, E. Garfunkel, Z. Bao, *Langmuir* **2004**, *20*, 1539–1542; e) A. M. Nowak, R. L. McCreery, *J. Am. Chem. Soc.* **2004**, *126*, 16621–16631; f) A. Jaiswal, K. G. Tavakoli, S. Zou, *Anal. Chem.* **2006**, *78*, 120–124; g) L. L. Zhao, L. Jensen, G. C. Schatz, *Nano. Lett.* **2006**, *6*, 1229–1234; h) R. L. McCreery, *Anal. Chem.* **2006**, *78*, 3490–3497.

[3] a) M. Fleischmann, P. J. Hendra, A. J. Mcquillan, *Chem. Phys. Lett.* **1974**, *26*, 163–166; b) D. L. Jeanmaire, R. P. Van Duyne, *J. Electroanal. Chem.* **1977**, *84*, 1–20; c) M. G. Albrecht, J. A. Creighton, *J. Am. Chem. Soc.* **1977**, *99*, 5215–5217; d) M. Moskovits, *Rev. Mod. Phys.* **1985**, *57*, 783–826; e) S. M. Nie, S. R. Emory, *Science* **1997**, *275*, 1102–1106; f) K. Kneipp, Y. Wang, H. Kneipp, L. T. Perelman, I. Itzkan, R. R. Dasari, M. S. Feld, *Phys. Rev. Lett.* **1997**, *78*, 1667;

g) H. X. Xu, E. J. Bjerneld, M. Käll, L. Börjessen, *Phys. Rev. Lett.* **1999**, *83*, 4357; h) K. A. Willets, R. P. Van Duyne, *Annu. Rev. Phys. Chem.* **2007**, *58*, 267–297; i) J. Kneipp, H. Kneipp, K. Kneipp, *Chem. Soc. Rev.* **2008**, *37*, 1052–1060; j) D. Y. Wu, J. F. Li, B. Ren, Z. Q. Tian, *Chem. Rev. Soc.* **2008**, *37*, 1025–1041.

[4] a) Q. Zhou, X. Li, Q. Fan, X. Zhang, J. Zheng, *Angew. Chem.* **2006**, *118*, 4074–4077; *Angew. Chem. Int. Ed.* **2006**, *45*, 3970–3973; b) Y. Wang, H. Chen, S. Dong, E. Wang, *J. Chem. Phys.* **2006**, *124*, 074709; c) G. Braun, I. Pavel. A. R. Morrill, D. S. Seferos, G. C. Bazan, N. O. Reich, M. Moskovits, *J. Am. Chem. Soc.* **2007**, *129*, 7760–7761; d) M. M. Maitani, D. A. A. Ohlberg, Z. Li, D. L. Allara, D. R. Stewart, R. S. Williams, *J. Am. Chem. Soc.* **2009**, *131*, 6310–6311.

[5] Y. Fang, N. H. Seong, D. D. Dlott, *Science* **2008**, *321*, 388–392.

[6] X. Wang, Z. Liu, M. D. Zhuang, H. M. Zhang, X. Wang, Z. X. Xie, D. Y. Wu, B. Ren, Z. Q. Tian, *Appl. Phys. Lett.* **2007**, *91*, 101105.

[7] a) T. Lu, T. M. Cotton, R. L. Birke, J. R. Lombardi, *Langmuir* **1989**, *5*, 406–414; b) A. Moissette, Y. Batonneau, C. Brémard, *J. Am. Chem. Soc.* **2001**, *123*, 12325–12334.

[8] A. Topaçli, S. Akyüz, *Spectrochim. Acta Part A* **1995**, *51*, 633–641.

[9] J. A. Larsson, M. Nolan, J. C. Greer, *J. Phys. Chem. B* **2002**, *106*, 5931–5937.

[10] G. Frens, *Nature Phys. Sci.* **1973**, *241*, 20–22.

[11] a) A. D. Becke, *J. Chem. Phys.* **1993**, *98*, 5648–5652; b) C. Lee, W. Yang, R. G. Parr, *Phys. Rev. B* **1988**, *37*, 785–789.

[12] P. C. Hay, W. R. Wat, *J. Chem. Phys.* **1985**, *82*, 299–310.

[13] D. Y. Wu, M. Hayashi, Y. J. Shiu, K. K. Liang, C. H. Chang, Y. L. Yeh, S. H. Lin, *J. Phys. Chem. A* **2003**, *107*, 9658–9667.

[14] Gaussian 03, Revision D, M. J. Frisch, G. W. Trucks, H. B. Schlegel, G. E. Scuseria, M. A. Robb, J. R. Cheeseman, J. A. Montgomery, Jr., T.Vreven, K. N. Kudin, J. C. Burant, J. M. Millam, S. S. Iyengar, J. Tomasi, V. Barone, B. Mennucci, M. Cossi, G. Scalmani, N. Rega, G. A. Petersson, H. Nakatsuji, M. Hada, M. Ehara, K. Toyota, R. Fukuda, J. Hasegawa, M. Ishida, T. Nakajima, Y. Honda, O. Kitao, H. Nakai, M. Klene, X. Li, J. E. Knox, H. P. Hratchian, J. B. Cross, V. Bakken, C. Adamo, J. Jaramillo, R. Gomperts, R. E. Stratmann, O. Yazyev, A. J. Austin, R. Cammi, C. Pomelli, J. W. Ochterski, P. Y. Ayala, K. Morokuma, G. A. Voth, P. Salvador, J. J. Dannenberg, V. G. Zakrzewski, S. Dapprich, A. D. Daniels, M. C. Strain, O. Farkas, D. K. Malick, A. D. Rabuck, K. Raghavachari, J. B. Foresman, J. V. Ortiz, Q. Cui, A. G. Baboul, S. Clifford, J. Cioslowski, B. B. Stefanov, G. Liu, A. Liashenko, P. Piskorz, I. Komaromi, R. L. Martin, D. J. Fox, T. Keith, M. A. Al-Laham, C. Y. Peng, A. Nanayakkara, M. Challacombe, P. M. W. Gill, B. Johnson, W. Chen, M. W. Wong, C. Gonzalez, . A. Pople, Gaussian, Inc., Wallingford CT, **2004**.

[15] a) K. S. Yee, *IEEE Trans. Antennas Propag.* **1966**, *14*, 302–307; b) K. S. Kunz, R. J. Luebbers, *The Finite Difference Time Domain Method for Electromagnetics*, CRC Press, Boca Raton, **1993**.

[16] P. B. Johnson, R. W. Christy, *Phys. Rev. B* **1972**, *6*, 4370–4379.

Received: August 6, 2009
Published online: December 22, 2009

